

A New Mixed Valent Europium Chloride: Na₅Eu₇Cl₂₂

Claudia Wickleder

Institut für Anorganische Chemie, Universität zu Köln,
Greinstrasse 6, D-50939 Köln, Germany

Reprint requests to Dr. Claudia Wickleder Fax: +49 (0)221 470 5083.

E-mail: claudia.wickleder@uni-koeln.de

Z. Naturforsch. **57 b**, 901–907 (2002); received April 23, 2002

Europium, Mixed Valence, Absorption Spectrum

The reaction of NaCl, EuCl₂ and EuCl₃ yields violet crystals of the new mixed valent chloride Na₅Eu₇Cl₂₂ which crystallizes with a hitherto unknown structure (orthorhombic, *Pmmm*, *Z* = 2, *a* = 2525.9(4), *b* = 846.91(9), *c* = 781.72(8) pm). The structure contains four crystallographically different europium ions, which can be attributed to Eu²⁺ or Eu³⁺ with respect to their coordination numbers and Eu-Cl distances. The [EuCl_x] coordination polyhedra are connected to chains along the [001] direction. Absorption spectra show transitions which can be assigned either to Eu³⁺ or Eu²⁺ ions or to *intervalence charge transfer transitions* (IVCT). The latter are at lower energy compared to other mixed valent europium chlorides. The occurrence of IVCT and the number of the crystal field levels of the Eu³⁺ ions reveal that the sites of the europium ions are occupied for a small amount by ions of the respective other valence.

Introduction

Mixed valent compounds are of special interest due to their unusual electronic properties [1]. Up to now most of the work on mixed valent materials focused on transition metal compounds. Mixed valent lanthanide halides should show exceptional behaviour when the electronic ground states are pure 4fⁿ states. Because these states have extremely narrow bands, localisation of the electrons occurs and their hopping between two ions is thermally induced. Additionally, more strongly ionic compounds cause small polarons [2]. This is illustrated by comparison of the Mößbauer spectra of Eu₃S₄ [3] and NaEu₂Cl₆ [4]. While the spectrum of the first compound shows delocalisation at room temperature and two peaks are observed at lower temperatures only, the barrier for NaEu₂Cl₆ is too high to allow thermal hopping at room temperature. Therefore, two peaks are detected. The respective *intervalence charge transfer transitions* (IVCT) of rare earth halides have been investigated only in the case of mixed Eu₄Cl₉/Eu₅Cl₁₁ crystals [5], where the interpretation is very difficult due to the many crystallographic positions for both ions. Very recently, absorption spectra were recorded for KEu₂Cl₆ and K_{1.6}Eu_{1.4}Cl₅ [6] which exhibit only one mixed valent site.

Ternary mixed valent lanthanide halides frequently crystallize with a filled variant of the UCl₃ type structure [6 - 8], as might be seen for NaEu₂Cl₆ and KEu₂Cl₆. On the other hand, the crystal structure of K_{1.6}Eu_{1.4}Cl₅ [6] was described as a substitution variant of the trivalent compounds K₂MCl₅ (M = La - Dy) [9].

During attempts to synthesize large samples of NaEu₂Cl₆ the deep violet phase Na₅Eu₇Cl₂₂ was obtained exhibiting an unknown structure. In this paper the results of the single crystal investigation are presented along with optical absorption measurements aiming for the investigation of transitions of the di- and trivalent ions and these to the intervalence charge transfer excited state.

Experimental Section

Na₅Eu₇Cl₂₂ was first obtained as a by-product during the preparation of NaEu₂Cl₆. The deliberate synthesis yielded a sample of Na₅Eu₇Cl₂₂ accompanied by small amounts of NaEu₂Cl₆. For this purpose oxide free EuCl₃ was prepared from Eu₂O₃ (Alpha, 99.9%) by the ammonium halide route [10]. A part of this sample was reduced to EuCl₂ in an Ar/H₂ gas stream at 650 °C. The binary chlorides NaCl (p. a., Merck), EuCl₂ and EuCl₃ were mixed in a molar ratio of 5 : 4 : 3, sealed in a silica ampoule under vacuum and heated to 500 °C followed by slow cooling (1 °C/h) using the Bridgman technique. The

Table 1. Crystallographic data of Na₅Eu₇Cl₂₂ and their determination.

Lattice parameters	$a = 2525.9(4)$ pm $b = 846.91(9)$ pm $c = 781.72(8)$ pm 503.58 cm ³ /mol
Molar volume	2
No. of formula units	2
Crystal system	orthorhombic
Space group	<i>Pmnn</i> (no. 59)
Diffractometer	Stoe IPDS I
Radiation	Mo-K _α (graphite monochrom., $\lambda = 71.07$ pm)
Temperature	293 K
Theta range	$5^\circ < 2\theta < 56^\circ$
Rotation range; increment	$0^\circ < \varphi < 200^\circ$; 2°
Index range	$-33 \leq h \leq 33$ $-11 \leq k \leq 11$ $-9 \leq l \leq 10$
No. of images	100
Exposure time	4 min
Detector distance	60 mm
Absorption correction	numerical after crystal shape optimisation [12]
μ	82.06 cm ⁻¹
Measured reflections	15632
Unique reflections	2216
— with $I_o > 2\sigma(I)$	1798
No. of variables	96
R_{int}	0.0741
Structure determinations	SHELXS-86 and SHELXL-93 [11]
Scattering factors	Intern. Tables, Vol. C [13]
Goodness of fit	1.008
$R1$; $wR2$ ($I_o > 2\sigma(I)$)	0.0338; 0.0694
$R1$; $wR2$ (all data)	0.0476; 0.0746
CSD no.	391121

main product contained deep violet crystals with diameters of up to $1 \times 1 \times 1$ mm³ and a few deep blue crystals of NaEu₂Cl₆ formed as a by-product. The sample is moisture sensitive and has to be handled in a glove box. Crystal specimens were selected and sealed in glass capillaries ($d = 0.1$ mm). To check their quality, several exposures were taken on an image plate X-ray diffractometer (STOE IPDS I), which was also used to collect diffraction data of the best specimen. The structure was solved and refined using the programs SHELXS-86 and SHELXL-93 [11], respectively. Absorption corrections were applied with the aid of the programs X-red and X-shape [12]. Crystallographic details are summarized in the Tables 1-3 and are additionally available from the Fachinformationszentrum Karlsruhe, D-76344 Eggenstein-Leopoldshafen (crysdata@FIZ-Karlsruhe.de) on quoting the deposition number given in Table 1.

The different colors of the Na₅Eu₇Cl₂₂ and NaEu₂Cl₆ crystals allowed a separation of the compounds in order

to get pure samples. For the absorption measurements a few crystals of Na₅Eu₇Cl₂₂ were selected, mixed with dried KBr and pressed to a pellet. The use of crystals was not possible due to their deep color even when the samples were cut and polished to very thin plates. Absorption measurements at room temperature and at low temperatures were performed using an absorption spectrometer (Cary 5e, Varian). Cooling to 12 K was achieved by a closed cycle helium cryostat (CS202, ADP Cryogenics).

Results and Discussion

Crystal structure

Na₅Eu₇Cl₂₂ crystallizes with an unknown crystal structure with two formula units per unit cell (Tab. 1, Fig. 1). The orthorhombic unit cell (space group *Pmnn*) offers four crystallographically different positions for the europium ions, which can be assigned to Eu²⁺ and Eu³⁺ with respect to their coordination numbers and Eu-Cl distances.

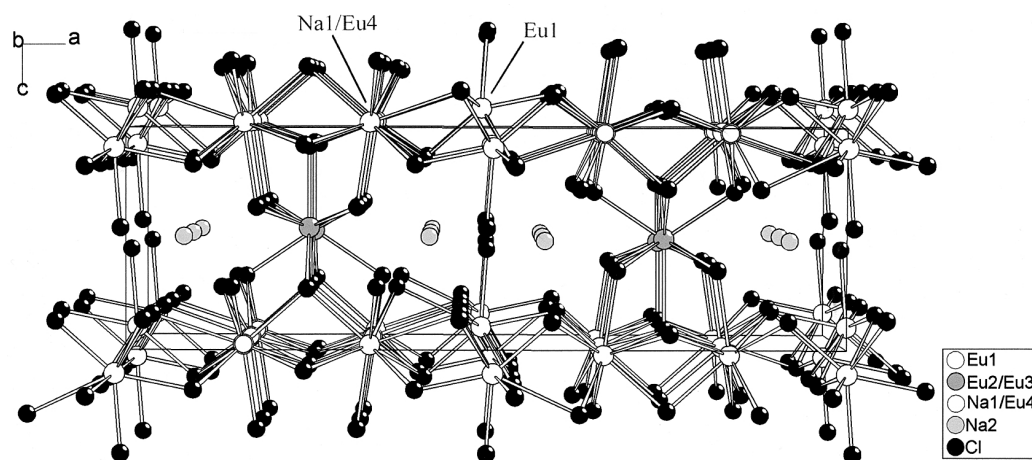
Eu(1) is sevenfold coordinated by Cl⁻ ions with Eu-Cl distances in the range 271 - 284 pm (Table 3). The values are comparable to those in Na₂EuCl₅. In the latter, the Eu³⁺ ions are also seven-coordinate with distances of 271 to 279 pm [15]. Hence, the position Eu(1) is mainly occupied by trivalent europium. The [Eu(1)Cl₇] polyhedra are connected via two common edges into zig-zag chains according to [Eu(1)Cl_{3/1}Cl_{4/2}] (Fig. 2).

In contrast, Eu(2) has coordination number nine and the Eu-Cl distances lie between 301 and 324 pm (Table 3), considerably longer than those of Eu(1), and thus can be assigned to Eu²⁺. The coordination polyhedron is a tricapped trigonal prism. For a comparison, EuCl₂ may be taken as a reference. It shows also ninefold coordination of Eu²⁺ (strictly speaking 7 + 2) and Eu-Cl distances of 292 - 344 pm [16]. Eu(3) is, like Eu(1), in sevenfold coordination of chloride ions in form of a monocapped trigonal prism with distances of 275 to 290 pm (Table 3). The distance to the prism cap (Eu-Cl: 290 pm) is remarkably larger than those to the vertices (275 and 277 pm). Obviously, this position is mainly occupied by Eu³⁺. The [Eu(2)Cl₉] and the [Eu(3)Cl₇] polyhedra are connected via a common face into dimers [Eu(2)Eu(3)Cl₁₃] which are further face-shared along the [010] direction to chains according to [Eu(2)Eu(3)Cl_{7/1}Cl_{6/2}] (Fig. 2).

Table 2. Atomic positions, site occupation factors (k) and equivalent isotropic displacement parameters for Na₅Eu₇Cl₂₂.

Atom	Site	Oxidationnumber	<i>x/a</i>	<i>y/b</i>	<i>z/c</i>	<i>k</i>	$U_{\text{eq}} \cdot 10^{-1}$ [pm ²]
Eu1	4 <i>f</i>	+3	0.50814(2)	1/4	0.08751(5)	1	16.4(1)
Eu2	2 <i>a</i>	+2	1/4	1/4	0.48938(7)	1	17.7(1)
Eu3	2 <i>b</i>	+3	1/4	3/4	0.45860(8)	1	31.2(2)
Eu4	8 <i>g</i>	+2	0.33741(1)	0.00187(4)	0.97646(5)	0.769(2)	21.2(1)
Na1	8 <i>g</i>	+1	0.33741(1)	0.00187(4)	0.97646(5)	0.231(2)	21.2(1)
Na2	8 <i>g</i>	+1	0.4199(1)	0.0029(4)	0.4906(4)	1	50(1)
Cl1	4 <i>e</i>	-1	1/4	0.9633(2)	0.7271(2)	1	19.6(4)
Cl2	4 <i>f</i>	-1	0.40086(8)	1/4	0.1596(3)	1	30.7(5)
Cl3	8 <i>g</i>	-1	0.31972(6)	0.9824(2)	0.3585(2)	1	25.3(3)
Cl4	8 <i>g</i>	-1	0.46260(7)	0.0492(2)	0.8362(2)	1	30.4(3)
Cl5	4 <i>f</i>	-1	0.34896(8)	1/4	0.7051(3)	1	25.1(4)
Cl6	4 <i>f</i>	-1	0.6271(1)	1/4	0.2689(4)	1	55.9(9)
Cl7	2 <i>b</i>	-1	1/4	3/4	0.0877(4)	1	34.1(7)
Cl8	4 <i>f</i>	-1	0.49972(8)	1/4	0.4411(3)	1	30.1(5)
Cl9	2 <i>a</i>	-1	1/4	1/4	0.0743(3)	1	23.1(6)
Cl10	4 <i>f</i>	-1	0.58876(9)	1/4	0.8571(3)	1	38.4(6)

$$U_{\text{eq}} = \frac{1}{3} [U_{11} + U_{22} + U_{33}] \text{ [14].}$$

Fig. 1. Perspective view of the crystal structure of Na₅Eu₇Cl₂₂ along [010].

One crystallographic position (8*g*) is occupied together by Eu(4) and Na(1). The occupation factors are 0.769(2) and 0.231(2), respectively (Table 2). Therefore, the composition of the crystal is Na_{4.924}Eu_{7.076}Cl₂₂. Even though X-ray diffraction techniques may not be the appropriate tool to determine the exact composition, a certain phase width can be assumed. Charge compensation is easy to achieve in any case by variation of the Eu²⁺/Eu³⁺ ratio. The Eu(4) and Na(1) ions are eightfold coordinated by Cl⁻ ions with distances between 296 and 319 pm (Table 3) close to typical values for Eu²⁺-Cl⁻ distances. Therefore it

can be assumed that this position is mainly occupied by Eu²⁺ rather than by Eu³⁺. The [Eu(4)Cl₈] and [Na(1)Cl₈] polyhedra, respectively, are connected via three common faces leading to double chains ∞ [MCl_{1/1}Cl_{5/2}Cl_{2/4}] along the [010] direction (Fig. 3).

Na(2) is eightfold (exactly: 6 + 2) coordinated by Cl⁻ ions with bicapped trigonal prisms as coordination polyhedra. The cation-chloride distances show a large variation between 274 and 347 pm (Table 3). These polyhedra are connected via common faces into chains ∞ [Na(2)Cl_{2/1}Cl_{6/2}] along the [010] direction (Fig. 3).

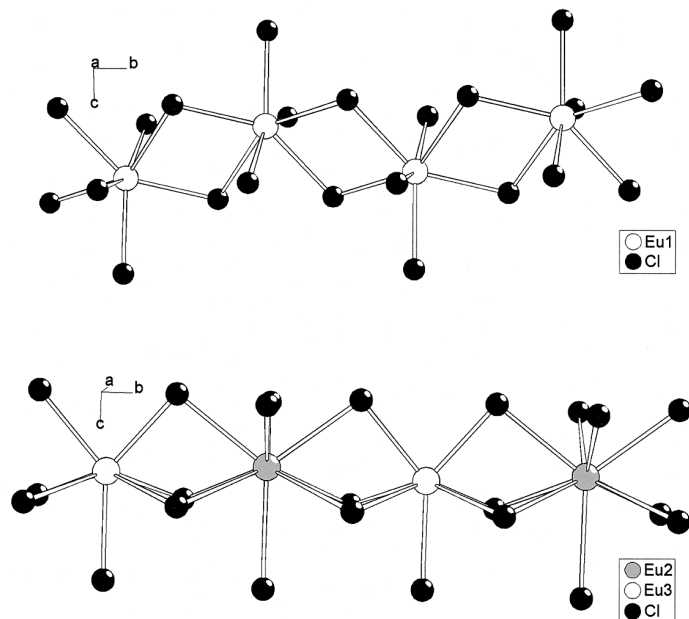


Fig. 2. $\frac{1}{\infty}[\text{Eu}(1)\text{Cl}_{3/1}\text{Cl}_{4/2}]$ (above) and $\frac{1}{\infty}[\text{Eu}(2)\text{Eu}(3)\text{Cl}_{7/1}\text{Cl}_{6/2}]$ (below) chains in the crystal structure of $\text{Na}_5\text{Eu}_7\text{Cl}_{22}$.

Table 3. Selected distances (pm) and angles ($^\circ$) for $\text{Na}_5\text{Eu}_7\text{Cl}_{22}$.

Eu1 - Cl4 (2x)	270.6(2)	Eu4/Na1 - Cl1	296.3(1)
- Cl10	271.9(2)	- Cl5	300.0(2)
- Cl2	276.8(2)	- Cl2	300.6(2)
- Cl8	277.3(2)	- Cl6	300.6(2)
- Cl4 (2x)	284.2(2)	- Cl3	302.5(2)
		- Cl10	311.8(2)
Eu2 - Cl5 (2x)	301.5(2)	- Cl9	314.2(1)
- Cl3 (4x)	304.7(1)	- Cl7	319.1(1)
- Cl1 (2x)	305.8(2)		
- Cl9	324.5(3)		
		Na2 - Cl3	273.8(3)
Eu3 - Cl3 (4x)	275.5(2)	- Cl8	293.2(3)
- Cl1 (2x)	276.9(2)	- Cl4	293.5(4)
- Cl7	289.9(3)	- Cl8	299.9(3)
		- Cl6	308.7(4)
		- Cl5	322.5(4)
		- Cl2	336.2(4)
		- Cl10	346.7(4)

The $\frac{1}{\infty}[\text{Eu}(1)\text{Cl}_{3/1}\text{Cl}_{4/2}]$ zig-zag chains are linked with the $\frac{1}{\infty}[\text{Eu}(4)/\text{Na}(1)\text{Cl}_{1/1}\text{Cl}_{5/2}\text{Cl}_{2/4}]$ double chains alternately via common edges and corners leading to layers parallel to the (001) plane (Fig. 1). These are connected in the [001] direction by $\frac{1}{\infty}[\text{Eu}(2)\text{Eu}(3)\text{Cl}_{7/1}\text{Cl}_{6/2}]$ chains in a way that each $\frac{1}{\infty}[\text{Eu}(3)\text{Cl}_7]$ polyhedron is connected to four $[\text{Eu}(4)/\text{Na}(1)\text{Cl}_8]$ polyhedra of one layer via common edges and to four $[\text{Eu}(4)/\text{Na}(1)\text{Cl}_8]$ polyhedra of another layer via common vertices. Furthermore,

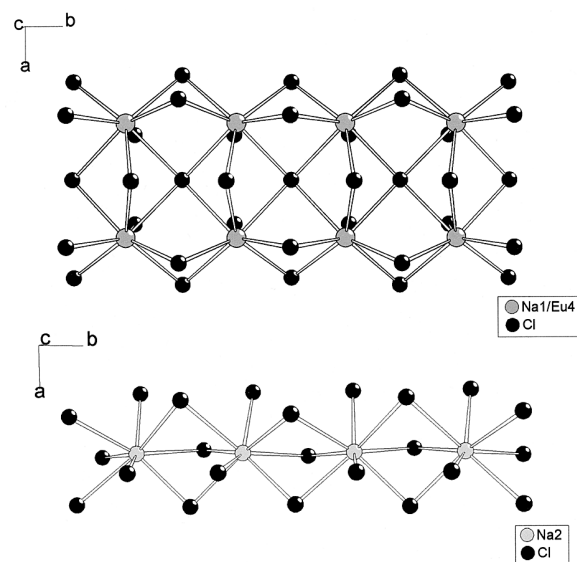


Fig. 3. $\frac{1}{\infty}[\text{Eu}(4)/\text{Na}(1)\text{Cl}_{1/1}\text{Cl}_{5/2}\text{Cl}_{2/4}]$ double chains (above) and $\frac{1}{\infty}[\text{Na}(2)\text{Cl}_{2/1}\text{Cl}_{6/2}]$ single chains (below) in the crystal structure of $\text{Na}_5\text{Eu}_7\text{Cl}_{22}$.

each $[\text{Eu}(2)\text{Cl}_9]$ polyhedron connects two layers via eight common edges. The Na(2) ions are located in the empty voids of this three-dimensional network (Fig. 1).

The structure is comparable to that of Na_2EuCl_5 (Fig. 4, [15]), although it is not simply a superstruc-

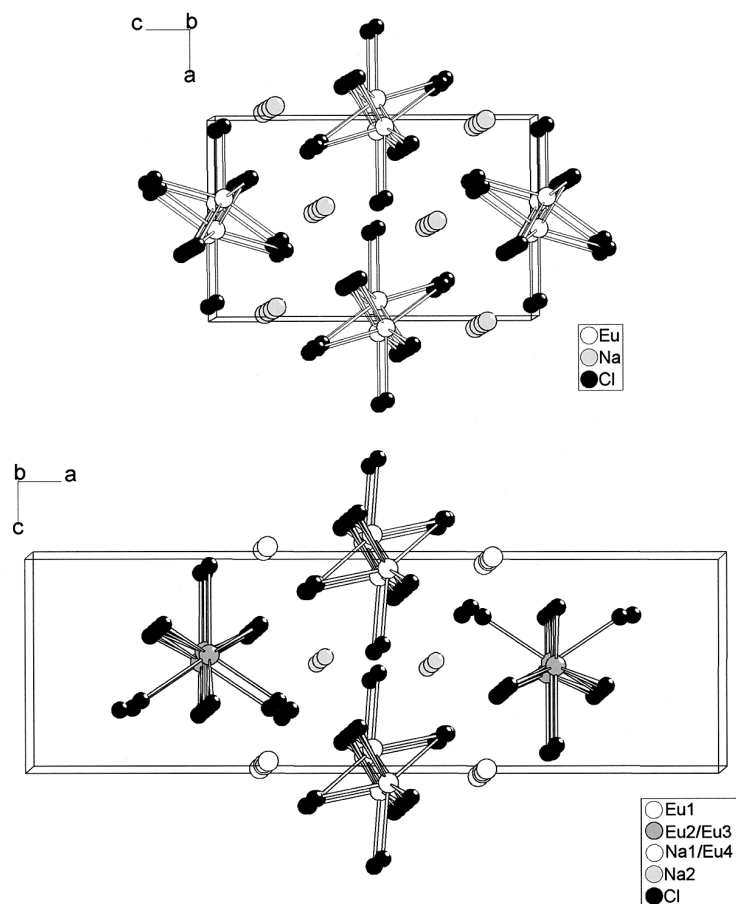


Fig. 4. Comparison of parts of the crystal structure of $\text{Na}_5\text{Eu}_7\text{Cl}_{22}$ (below) with the crystal structure of Na_2EuCl_5 (above).

ture. As mentioned above, the coordination polyhedra of Eu^{3+} in Na_2EuCl_5 and of $\text{Eu}(1)$ in $\text{Na}_5\text{Eu}_7\text{Cl}_{22}$ are very similar. The positions of the Na^+ ions are substituted either for $\text{Na}(2)$ or for $\text{Eu}(4)/\text{Na}(1)$ in $\text{Na}_5\text{Eu}_7\text{Cl}_{22}$.

Optical properties

Mixed valent compounds are distinguished by their intensive colors if the surroundings of the cations of different oxidation states are equal or at least similar. A configuration coordinate diagram with two potentials can be drawn with respect to the different distances of the cations to the ligands (Fig. 5). In the case of equal point symmetries a splitting Δ at the potential crossing point will occur, resulting in a ground state potential and an excited state potential at higher energy. Depending on the degree of splitting, the ground state potential yields

either an average oxidation state $[(m+n)/2]^+$ of the cations for a large splitting Δ_1 or two oxidation states for a small splitting Δ_2 . In the latter case the electron hopping is thermally initialized. In the case of rare earth chlorides it is expected that the splitting is extremely small because the 4f electrons are located close to the nuclei and the bonds are rather ionic. The energy difference of the ground state to the higher potential ΔE_{opt} is in most cases in the visible region of the electromagnetic spectrum. The transitions, the so called *intervalence charge transfer transitions* (IVCT), are strong, causing the deep color of the compounds.

The absorption spectra of $\text{Na}_5\text{Eu}_7\text{Cl}_{22}$ at 12 K are shown in Fig. 6. Three different kinds of transitions are present. A broad band which covers the whole visible range is observed with a maximum at 16030 cm^{-1} (for 298 K) and at 15970 cm^{-1} (for 12 K), respectively. The full width at half maximum

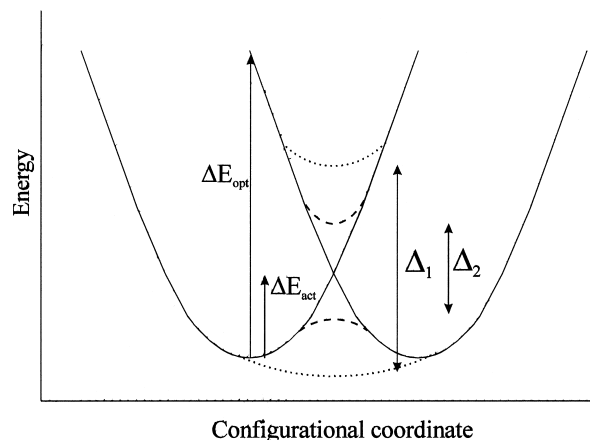


Fig. 5. Configurational coordinate diagram of a mixed valence compound with large splitting Δ_1 (···) and small splitting Δ_2 (- - -). ΔE_{opt} displays the energy of the intervalence charge transfer transition, ΔE_{act} those of the barrier.

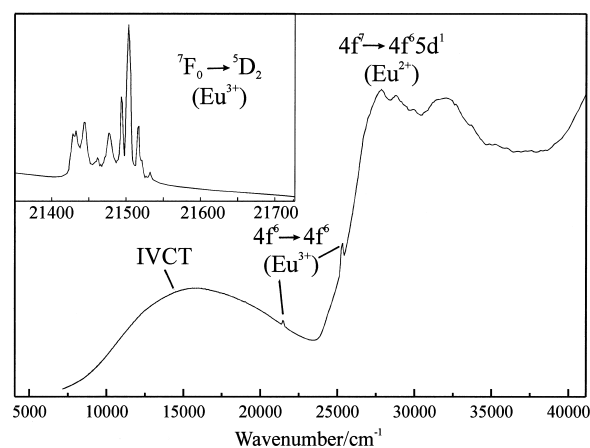


Fig. 6. Absorption spectrum of $\text{Na}_5\text{Eu}_7\text{Cl}_{22}$ at 12 K. The respective transitions are marked. The inset shows a high resolution spectrum of ${}^7\text{F}_0 \rightarrow {}^5\text{D}_2$ peaks of Eu^{3+} ions.

is $\nu_{1/2} = 12040 \text{ cm}^{-1}$ at 12 K. This band can be assigned to the IVCT transition. Even if the results of the X-ray structure analysis do not show any indication that one site is occupied by both Eu^{2+} and Eu^{3+} , the optical spectra point out that there must be a small amount of the other valence on at least one site. The amount is, of course, below the detection limit of X-ray diffraction methods.

In the case of small polarons, thermal hopping occurs close to the crossing points of the two parabolic curves. Thus, it is possible to estimate the energy of the potential barrier ΔE_{act} (Fig. 5), which is a quar-

ter of the energy of the optical transition [2], e. g. $\approx 4000 \text{ cm}^{-1}$ for $\text{Na}_5\text{Eu}_7\text{Cl}_{22}$. Assuming a Boltzmann distribution, the population of the vibrational levels with an energy of $E_{\text{vib}} = 4000 \text{ cm}^{-1}$ is $N_E/N_{\text{tot}} = 4 \cdot 10^{-9}$ at room temperature. Of course, this is only a rough estimation, because there is a decrease of the barrier due to the splitting. But even with half of the energy of the barrier, the amount of electrons possessing the thermal energy necessary for electron hopping will be small and it can be assumed that Mößbauer spectra will also show two peaks at room temperature as for NaEu_2Cl_6 [4].

Compared to IVCT bands of other europium chlorides, the maximum is red shifted to lower energies. The maxima of other bands are at 17240 cm^{-1} in KEu_2Cl_6 and at 18870 cm^{-1} in $\text{K}_{1.6}\text{Eu}_{1.4}\text{Cl}_5$ [6]. Even $\nu_{1/2}$ is larger than in the other compounds investigated ($\nu_{1/2} = 11180 \text{ cm}^{-1}$ in KEu_2Cl_6 [6]). This indicates that several mixed valent sites exist in $\text{Na}_5\text{Eu}_7\text{Cl}_{22}$, and that the observed band is a superposition of the transitions of all these sites. A more detailed inspection of Fig. 6 shows that the peak is not of Gaussian shape as it is expected for a single IVCT band. The maximum in $\text{Eu}_4\text{Cl}_9/\text{Eu}_5\text{Cl}_{11}$ mixed crystals is at comparable energy ($\nu_{\text{max}} = 16000 \text{ cm}^{-1}$ [5]), where several mixed valence sites are also found, so that a superposition of many transitions can be assumed.

Some additional broad bands in the ultraviolet region are detected (Fig. 6) which can be assigned to the parity allowed strong $4f^7 ({}^8\text{S}) \rightarrow 4f^6 5d^1$ transitions of Eu^{2+} ions. It is again a superposition of several bands due to the two Eu^{2+} sites each of which has five $4f^6 5d^1$ excited states due to the crystal field splitting of the 5d levels. The absorption maximum of the first transition is at 27850 cm^{-1} which is comparable to the respective maxima of Eu^{2+} ions doped in chloride host lattices [17]. The minimum of the absorption is at 23365 cm^{-1} (428 nm). In the visible range only the violet part is reflected, in contrast to KEu_2Cl_6 which shows a blue color and a minimum at 22220 cm^{-1} (450 nm) [6].

Some small peaks due to $4f^6 \rightarrow 4f^6$ transitions, e. g. ${}^7\text{F}_0 \rightarrow {}^5\text{D}_1$, ${}^7\text{F}_0 \rightarrow {}^5\text{D}_2$ and ${}^7\text{F}_0 \rightarrow {}^5\text{L}_6$, of the Eu^{3+} ions are also observed. In contrast to the $f \rightarrow d$ transitions of Eu^{2+} their energetic position is nearly independent of the lattice. The inset of Fig. 6 shows a high resolution spectrum of the ${}^7\text{F}_0 \rightarrow {}^5\text{D}_2$ transition. At least ten peaks can be observed which can be attributed to transitions to different crystal field

levels. While 7F_0 is a single state, 5D_2 is five-fold degenerate in the free ion. In crystals this degeneracy is removed. The number of crystal field levels is determined by the point symmetry of the crystallographic site. While Eu^{3+} ions on the 4f sites (point symmetry C_s) or 8g sites (C_1) would have a five-fold splitting, for Eu^{3+} ions on the sites 2a (C_{2v}) or 2b (C_{2v}) four crystal field levels can be observed [18]. Therefore, if only Eu(1) and Eu(3)

would be occupied by Eu^{3+} , nine levels would be detected at most. The detection of ten levels reveals that one or more of the small peaks are due to the occupation of the Eu(2) or Eu(4) sites by small amounts of Eu^{3+} .

Acknowledgement

The author is indebted to Prof. Dr. G. Meyer for generous support.

-
- [1] K. Prassides (Ed.), *Mixed Valency Systems: Applications in Chemistry, Physics and Biology*, NATO ASI Series C, Vol. 343, Kluwer Academic Publishers, Dordrecht, Boston, London (1991).
- [2] P. A. Cox, *The Electronic Structure and Chemistry of Solids*, Oxford Science Publication, Oxford (1987).
- [3] O. Berkooz, M. Malamud, S. Shtrikman, *Solid State Commun.* **6**, 185 (1968).
- [4] K. D. Becker, C. Wickleder, unpublished.
- [5] F. T. Lange, Dissertation, Universität Karlsruhe, 1992.
- [6] C. Wickleder, *Z. Anorg. Allg. Chem.*, accepted for publication.
- [7] M. S. Wickleder, G. Meyer, *Z. Anorg. Allg. Chem.* **622**, 593 (1996).
- [8] M. S. Wickleder, G. Meyer, *Z. Anorg. Allg. Chem.* **624**, 1577 (1998).
- [9] G. Meyer, E. Hüttel, *Z. Anorg. Allg. Chem.* **497**, 191 (1983); G. Meyer, J. Soose, A. Moritz, V. Vitt, Th. Holljes *Z. Anorg. Allg. Chem.* **521**, 161 (1985).
- [10] G. Meyer, *Inorg. Synth.* **22**, 1 (1983).
- [11] G. M. Sheldrick, SHELXS-86, Programs for X-ray structure analysis, Göttingen (1986); G. M. Sheldrick, SHELXL-93, Program for the Refinement of Crystal Structures, Göttingen (1993).
- [12] X-RED 1.07, Data Reduction for STADI4 and IPDS, Stoe & Cie Darmstadt 1996; X-SHAPE 1.01, Crystal Optimisation for Numerical Absorption Correction, Stoe & Cie Darmstadt (1996).
- [13] Th. Hahn (ed.), *International Tables for Crystallography*, Vol. C, D. Reidel Publishing Company, Dordrecht, Boston (1983).
- [14] R. X. Fischer, E. Tillmanns, *Acta Crystallogr.* **C44**, 775 (1988).
- [15] M. S. Wickleder, G. Meyer, *Z. Anorg. Allg. Chem.* **621**, 740 (1995).
- [16] H. Bärnighausen, *Rev. Chim. Mineral.* **10**, 77 (1973).
- [17] J. Rubio O., *J. Phys. Chem. Solids* **52**, 101 (1991).
- [18] C. Görller-Walrand, K. Binnemans, *Rationalization of crystal-field parametrization*, in: *Handbook on the Physics and Chemistry of Rare Earth*, Vol. 23, ch. 155, 121, North-Holland, Amsterdam (1996).